Although the measurement and evaluation of cutting temperature in machining processes are very important, not all techniques are equally effective or just as simple when it comes to performing them [7]. Some difficulties that may be encountered in measurement processes are proper environmental conditions and different thermal emissivity on the surfaces of the tool and the workpiece if measurement methods are based on this property [8, 9].

Cutting machining processes temperatures can be estimated by several analytical methodologies. One of the most widely used ones is Cook's method, which predicts the temperature values at the tool-chip interface in a machining process [1, 10].

However, these temperature values and their distribution in the machined area can be determined by several techniques, such as thermocouples or infrared thermography.

Grzesik [11] used a K-type thermocouple inserted into the workpiece to know the interfacial temperature in a machining operation. Other authors have used thermocouples to develop different temperature analysis methods. By these devices, Richardson *et al*. [12], implemented an analytical approach to predict machining-induced workpiece temperatures. Their model allowed them to know the magnitude and distribution of temperatures in the workpiece in a dry milling process.

Kuczmaszewski and Zagorski [13] analyzed the effectiveness of these different methods for measuring temperature in the cutting zone. They concluded that the use of thermocouples was not suitable for those cases in which the cutting depth was not very deep and were, thus, of hardly any use under real industrial conditions. Otherwise, a method based on an infrared thermographic camera is more suitable for measuring temperature values in machining operations. Pittala and Monno [14] used an infrared camera to record and measure the temperature of a part in a milling operation. An operation of this type is based on infrared thermography, a technique used for measuring the temperature of objects as they all emit infrared radiation if the temperature is above 0 K [15]. The application of this method has extended to industrial applications, research and development as it is possible to take real-time measurements without having to come into contact with the object [16]. The operating fundamentals of this procedure can be understood as so: any object emits thermal energy according to its temperature as infrared, which converges on the camera´s electronic detector, and brings about changes in output voltage or electrical resistance, which are read by the camera's chip. This electronic signal is turned into an image that is displayed on the camera screen [17].

To ensure correct camera operation, some parameters have to be taken into account, such as room temperature, relative humidity, object distance, and the emissivity of the material [13].

The emissivity of any material could be affected if work is being done within a wide temperature range. Thus, it is necessary to establish a process to know the actual emissivity of the material under certain conditions.

The importance of emissivity can be understood if the definition of a blackbody is considered. A blackbody is an ideal body that absorbs all the energy of an infrared radiation incident upon it, converts it into infrared radiation and emits it all. A blackbody's emissivity eq. (1), thus reflection or transmission of radiation does not occur. Consequently, this kind of body is used to calibrate infrared procedure [18].

According to Kirchhoff's law, the radiation emitted and absorbed by a real body are in thermal equilibrium; that is, an object always emits exactly the same amount of heat that it receives. Thus the amount of radiation which emanates from an object comes as three different types: emitted radiation ($W_\varepsilon$), reflected radiation ($W_\rho$) and transmitted radiation ($W_\tau$), [15], as shown in eq. (1):

$$W_{emanating} = W_{\varepsilon} + W_{\rho} + W_{\tau} \tag{1}$$

Emitted radiation, $W_{\varepsilon}$, is the most important type in the thermography technique. The ability of an object to send out its own energy as radiation depends mainly on its emissivity, ε. The emissivity value is the ratio between the radiation emitted by a real body ($W_{RB}$) and the radiation emitted by a blackbody ($W_{BB}$), as seen in eq. (2). The evaluation made by an infrared camera is based on eq. (2):

$$\varepsilon = \frac{W_{RB}}{W_{BB}} \tag{2}$$

Research about cutting temperatures in milling processes is lacking because this kind of operation is non-steady and some measuring difficulties related to temperature variation with the time can be encountered. Nor is it easy to monitor temperature measurements [5]. In this paper, a methodology for cutting temperature measurements in milling processes was carried out using infrared thermography. For this purpose, the emissivity of the materials under different conditions was established. Moreover, an evaluation and an analysis of the different milling cutting parameters, and of their influence on the temperatures generated during faced milling, were performed.

## Experimental details and procedures

Conventional milling tests (workpiece in the opposite direction of the rotation tool) were carried out on three materials, EN AW-2007 aluminum alloy, ETP-300 electrolytic copper and AISI 304 stainless steel. Thermal conductivity properties were very different in all these materials and their respective values were 130, 393, and 16.7 W/mK.

All the front milling tests were performed on a CNC vertical machining center using a HSS tool with a titanium-aluminum nitride (TiAlN) coat without lubrication; that is, under dry conditions.

A SATIR infrared camera (model Hotfind-LXT) was used to record cutting temperatures. This device is monitored with specific software, which allows the selection of the areas in which the temperature must be determined. A special support to fix the camera in a constant position, approximately 400 mm from the workpiece, was designed.

A process, which we usually apply in the thermographic area, was run to perform an appropriate adjustment of emissivity and to guarantee correct thermographic camera operation. The emissivity value is necessary to be properly introduced into the supporting software to obtain correct temperature readings. To this end, a workpiece of dimensions 100 mm × 100 mm × 12 mm was placed inside an oven to raise its temperature to approximately 50 °C. The workpiece had a black painted area, which was recorded after heating simultaneously with the infrared camera and a thermocouple during the cooling period. Thus cooling curves were obtained and compared to fix the correct emissivity value for the selected painted area on the material. As expected, the value of this is emissivity, $\varepsilon$, came close to 0.95.

To determine the emissivity value of each material under the specific test conditions, a preliminary milling test was carried out by taking the temperature in the black area as a reference, fig. 1. With this value, the emissivity that corresponded to the bare area was adjusted to obtain the same temperature value.

We can see that the differences between both surface types are remarkable. Note in fig. 1 that the main part of the incident radiation was absorbed by the black surface. Nevertheless, the bare surface reflected a large amount of incident radiation and, if emissivity was not

correctly adjusted, it would lead the thermographic camera to record a false temperature value. Thus, emissivity results were established as 0.773 for aluminum alloy, 0.879 for copper and 0.921 for stainless steel.

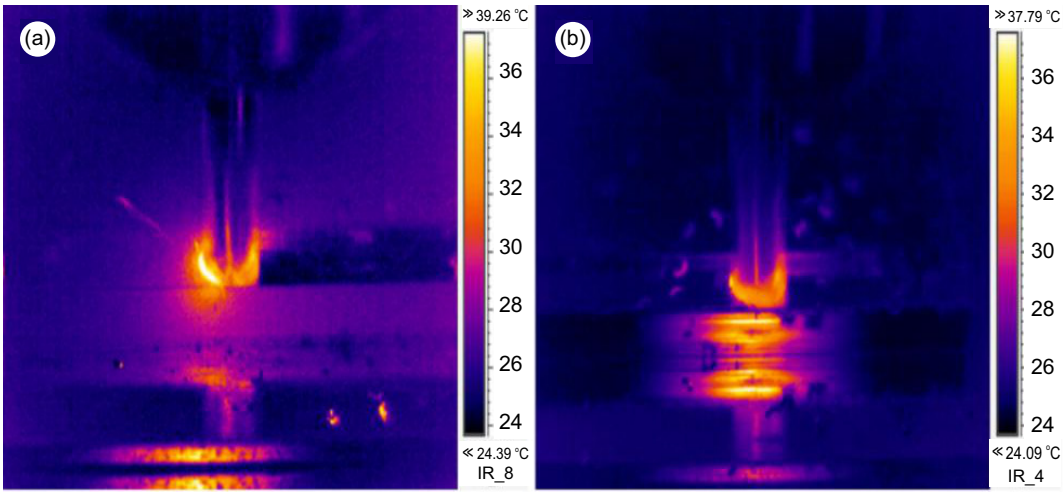


**Figure 1. Thermal images in copper ETP-R300 milling; black painted area (a), bare zone (b)**
(*for color image see journal web site*)

### *Cutting parameters*

Cutting tests were run after taking the different machining parameters into account, such as spindle speed, $N$, feed per tooth, $fz$, axial depth of cut, $a_p$, and radial depth of cut, $a_e$. The camera was fixed to the table of the milling machine. Thus, its position respect to the tool did not change during the machining test, fig. 2(a).

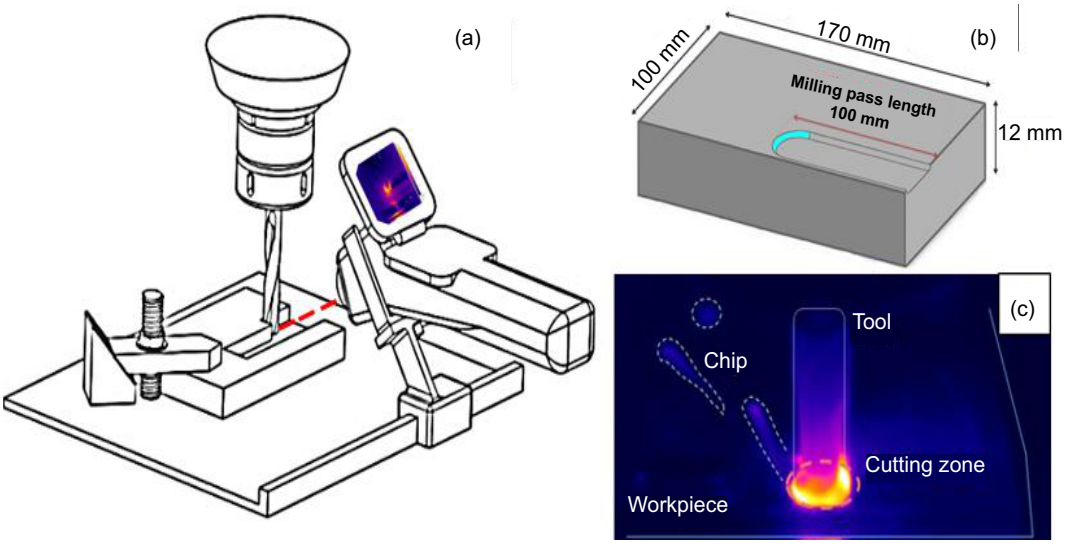


**Figure 2. (a) position of the camera, tool, and workpiece, (b) schematic view of a sample cutting test, (c) example of the thermal image of a workpiece obtained with some details during milling**
(*for color image see journal web site*)

Every milling operation was defined as a single pass of 100 mm long, and was carried out according to the aforementioned parameters, fig. 2(b). The three analyzed materials were machining under similar conditions. The experimental values established for the milling operations are shown in tab. 1.

**Table 1. Cutting parameters that correspond to face milling operations**

| Test | Spindle Speed [rpm] | Feed per tooth [mm per tooth] | Axial Depth [mm] | Radial Depth [mm] |
|---|---|---|---|---|
| EN AW-2007 aluminum alloy | | | | |
| 1-6 | 500 / 3000 (500 step) | 0.075 | 1 | 10 |
| 7-11 | 2000 | 0.025 / 0.125 (0.025 step) | 1 | 10 |
| 12-15 | 2000 | 0.075 | 0.25 / 1 (0.25 step) | 10 |
| 16-19 | 2000 | 0.075 | 1 | 2.5 / 10 (2.5 step) |
| ETP-R300 copper | | | | |
| 1-6 | 500 / 3000 (500 step) | 0.035 | 0.5 | 10 |
| 7-11 | 2000 | 0.015 / 0.055 (0.01 step) | 0.5 | 10 |
| 12-15 | 2000 | 0.035 | 0.25 / 1 (0.25 step) | 10 |
| 16-19 | 2000 | 0.035 | 0.5 | 2.5 / 10 (2.5 step) |
| AISI 304 stainless steel | | | | |
| 1-6 | 500 / 3000 (500 step) | 0.02 | 0.25 | 10 |
| 7-12 | 2000 | 0.01 / 0.035 (0.005 step) | 0.25 | 10 |
| 13-16 | 2000 | 0.02 | 0.25 / 1 (0.25 step) | 10 |
| 17-20 | 2000 | 0.02 | 0.25 | 2.5 / 10 (2.5 step) |

### *Analytical procedures for estimating cutting temperature*

As far as the authors know, there is almost no literature available on analytical methods to determine cutting temperatures in milling operations. One of the most widespread general equations is Cook's, eq. (3). This expression predicts the mean temperature, $\Delta T$, at the tool-chip interface according to the specific energy of the operation, $U$, the density and heat coefficient of the material, $\rho$, and $C$, respectively, and to the cutting speed, $V_c$, the initial chip thickness, $t_o$, and the thermal diffusivity of the workpiece, $K$. The cutting interface temperature must be obtained by adding room temperature to $\Delta$T [19]:

$$\Delta T = \frac{0.4U}{\rho C}\left(\frac{\nu C t_o}{K}\right)^{0.333} \tag{3}$$

Specific energy and thermal diffusivity take different values according to the material, and are published in the literature. Depending on the source, different, but similar, values are found [1, 2]. In any case, in this work a mean value was considered for each material, as indicated in tab. 2. The mechanical properties of the material were also established, tab. 2.

**Table 2. Properties of the studied materials**

| | EN AW-2007 Aluminum alloy | ETP-R300 Copper | AISI 304 Stainless steel |
|---|---|---|---|
| Specific energy, [Jmm$^{-3}$] | 0.8 | 1.4 | 2.8 |
| Thermal diffusivity, [Wm$^{-1}$ ºC$^{-1}$] | $5.33 \cdot 10^{-5}$ | $1.14 \cdot 10^{-4}$ | $4.21 \cdot 10^{-6}$ |
| Yield strength, [MPa] | 295-360 | 68-294 | 210-240 |
| Tensile strength, [MPa] | 445-460 | 300 | 520-585 |

## Results and discussion

Milling cutting temperatures were measured after taking into account a specific area of the thermographic image, as shown in fig. 2(c). The thermographic camera scanned a relatively small cutting zone, which resulted in temperature data collection. As seen in fig. 2(c), the temperature in the contact tool-workpiece, an area very close to the cutting interface, was almost uniform. Chip rapidly cools, as expected, if the thermal fundamentals of cutting processes are taken into account [20]. Thus different consecutively recorded temperature values hardly ranged between 10 ºC, as represented in fig. 3. This figure also shows the time range of the temperature measurements corresponding to the whole feed rates involved in the machining tests. As milling is an interrupted cutting process, slight variation in temperature might be attributed to this circumstance. Moreover, camera readings were taken as the mapping of a small selected area and, accordingly, some differences in temperature values appeared.

To facilitate the interpretation of the temperature results, an average value of about 50 consecutive readings was obtained, and logarithmic regression was done to obtain a good correlation, $R$, for aluminum and stainless steel machining (above 0.85). This correlation was poorer for copper. Figure 4 shows these simplified temperature functions after taking into account that the only variable considered in it was spindle speed; that is, cutting velocity. Thae adjustments made to the high spindle speed values revealed that a milling length of 100 mm may not be enough to stabilize temperature in the machining operation. However, the real temperature data collection representation in fig. 3 shows that the cutting temperature results are considered to come close to the mean value.

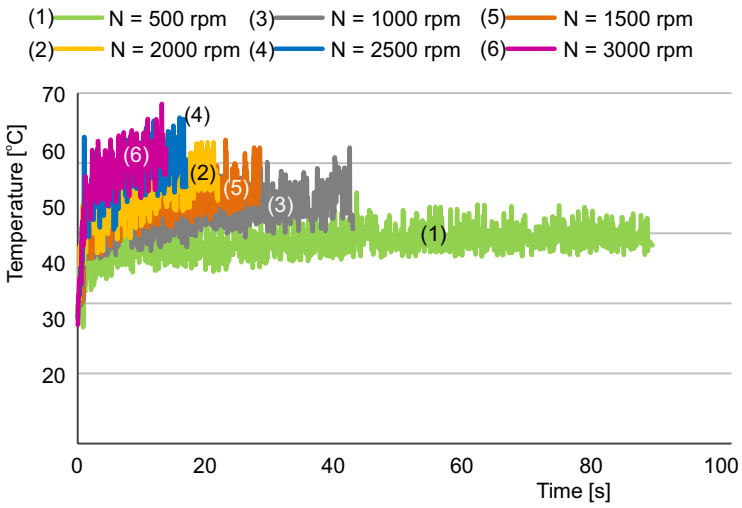


**Figure 3. Example of real temperature data collection of a milling process of an aluminum alloy workpiece by varying spindle speed; machining parameters: $fz$ = 0.075mm/tooth, $a_p$ = 1, $a_e$ = 10mm**

In all cases, cutting temperature quickly increased for the high-speed values. The slightest temperature variations were associated with ETP-R300 electrolytic copper. This material obtained the highest thermal diffusivity coefficient, which means

that it was hardly heated in milling processes. AISI 304 stainless steel was found on the other extreme as it was the material with the lowest heat transfer coefficient. Therefore it underwent significant temperature changes, depending on the spindle speed value. Logically, the temperature values for aluminum were in an intermediate position between the above-mentioned materials. Plasticity differed for the experimented materials according to its yield strength and strain hardening index [21]. Once again stainless steel involved the strongest machining energy, as reflected by its highest specific cutting energy value [2].

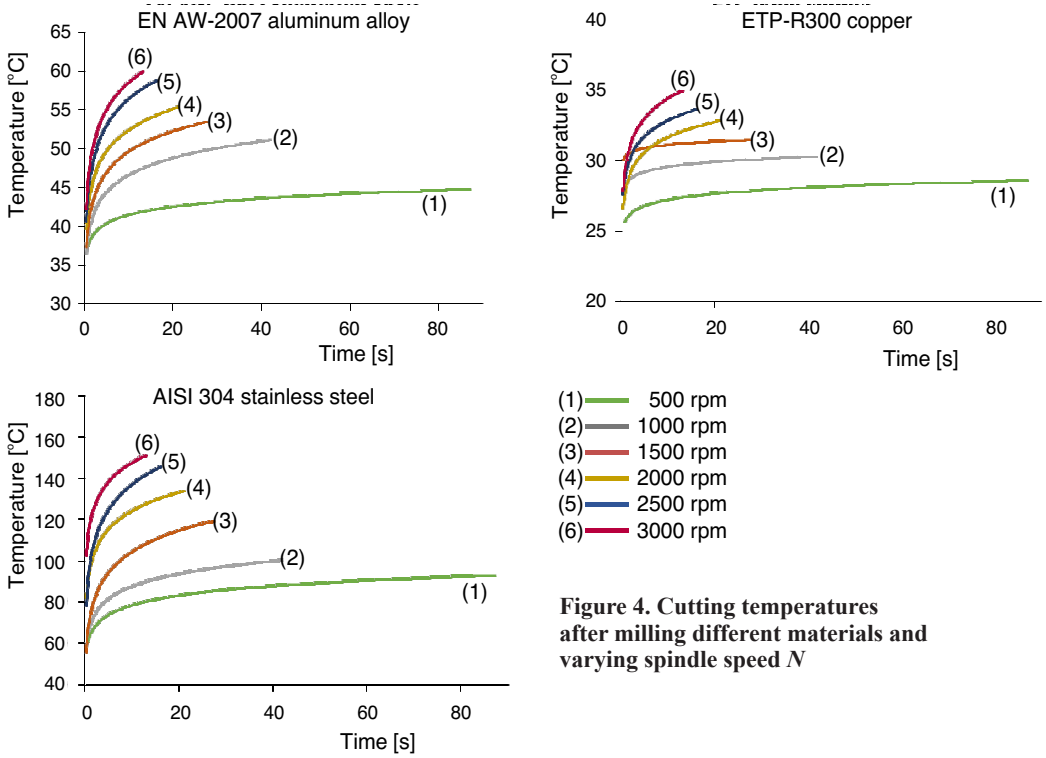


**Figure 4. Cutting temperatures after milling different materials and varying spindle speed *N***

In order to simplify the comparison made between the different tests, cutting average temperature values and standard deviation were obtained by considering the last 25 mm of the milling operation, fig. 5, as it was assumed that cutting temperature was almost stabilized in this length. Figure 5 represents the average cutting temperatures in the milling processes by varying the different machining parameters. Standard deviation was also obtained to verify if major temperature fluctuations took place in the different studied milling operations.

According to the results, standard deviation had a significant purpose in the stainless steel tests in which cutting temperature values fluctuated because of the heat transfer conditions conferred by the material. The standard deviations for the tests performed on the other materials were not significant since all the recorded temperature values came very close to the average calculated value, which is not represented in fig. 5. The temperature results obtained herein were comparable to those reported by other authors for similar machining conditions [22].

AISI 304 stainless steel achieved higher cutting temperature results when any cutting parameter value was increased. In fact, spindle speed was the most influential factor. EN AW-2007 aluminum alloy and ETP-R300 electrolytic copper varied only slightly from different milling conditions.

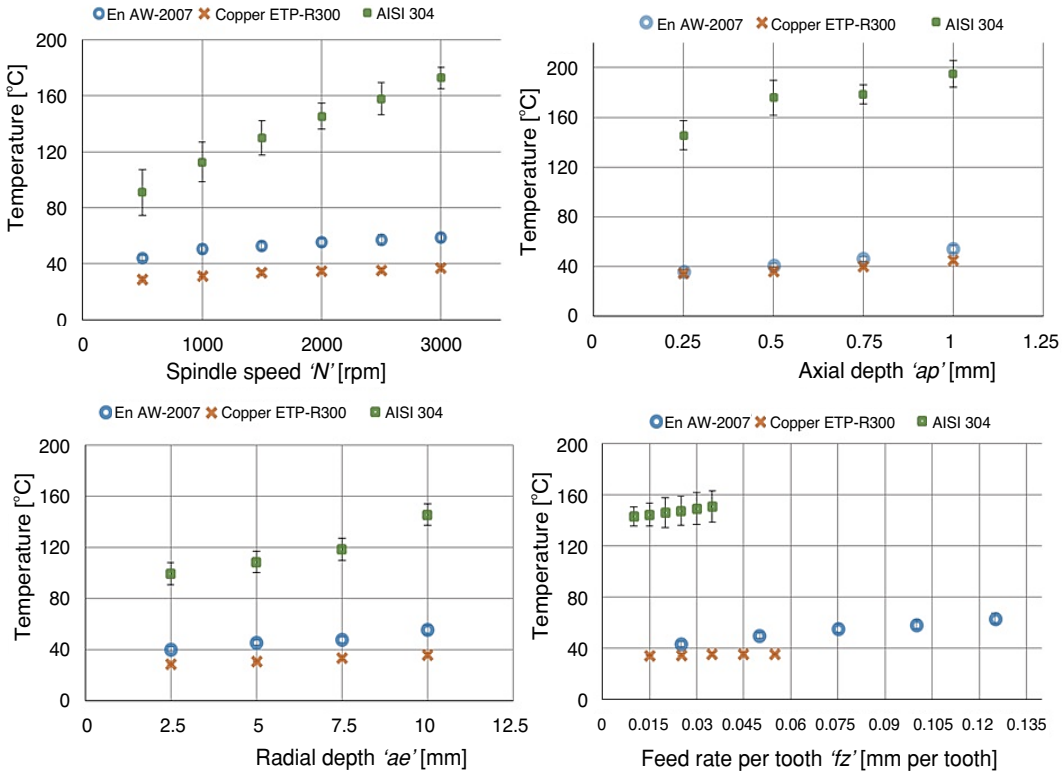


**Figure 5. Average cutting temperatures in milling processes by varying spindle speed, axial depth, radial depth and feed rate per tooth**

## Analytical considerations of cutting temperature

After analyzing the experimental temperature results, Cook's analytical method was applied to obtain the theoretical cutting temperature values after taking into account the same cutting conditions as those used in the milling operations. Figure 6 depicts the experimental and theoretical cutting temperature values. Each graph represents all the tests carried out with the different studied materials according to tab. 2. As seen, eq. (3), Cook's equation, did not depend on radial and axial depth as the expression did not involve these variables. Thus the temperature prediction for the last eight tests was constant.

This assertion is at least controversial if we contemplate some energetic models [21] that are coherent with the experimental results obtained herein. As observed in fig. 6, axial and radial depth influenced cutting temperature, which was more noticeable for stainless steel milling.

In short, the theoretical and experimental results behaved differently according to the type of material being machining. When comparing graphs, the recorded temperatures differed vastly from the theoretical results for AISI 304 stainless steel.

## Conclusions

The use of infrared thermography for measuring cutting temperatures proved to be a reliable and valid method. However, it is necessary to bear in mind the difficulty of measuring

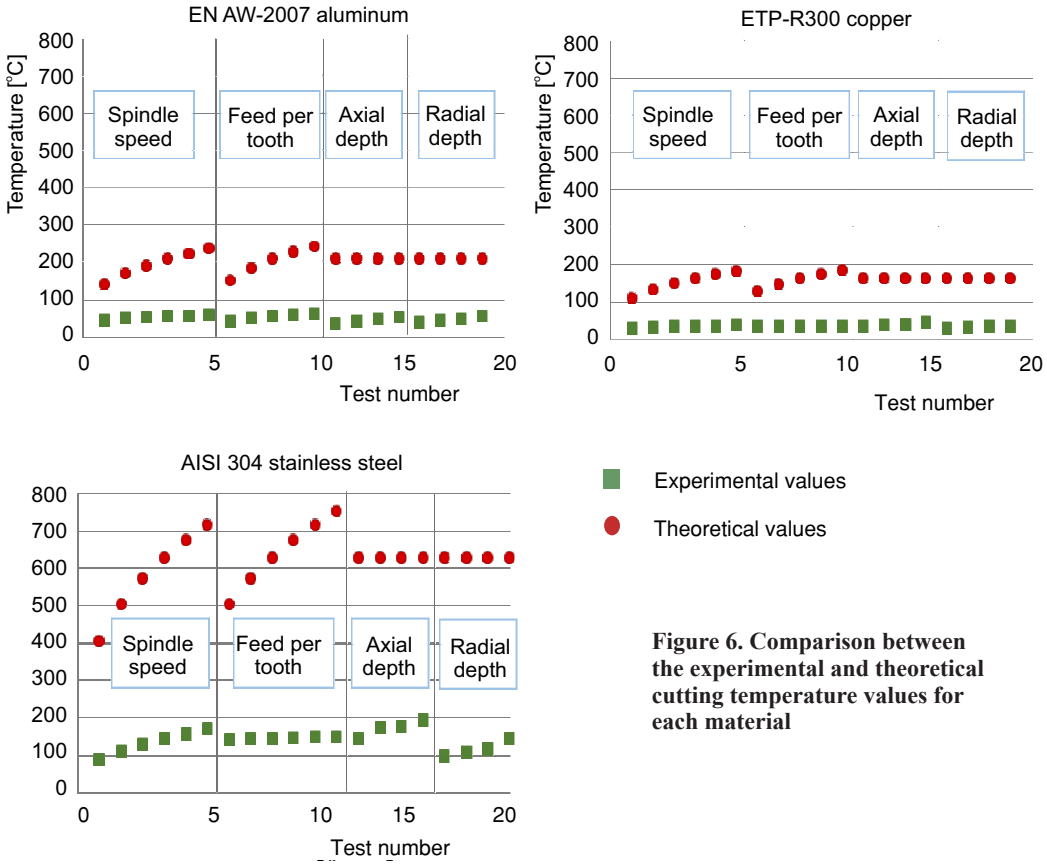


**Figure 6. Comparison between the experimental and theoretical cutting temperature values for each material**

on metals given their emissivity values and their strong reflection power. A remarkable acceptable methodology for calculating the emissivity of metals was achieved, which is presented in this research work to help overcome such problems.

A direct relationship was observed between cutting temperatures and machining parameter values. Analytical methods proved questionable as the obtained results depended very much on intrinsic material parameters, which are difficult to obtain, as are specific machining conditions, and were not considered in the equations or did not allow the results to be extrapolated to the different method situations. Thus Cook's equation has been employed by different authors without considering relevant parameters such as cutting depth.

The parameters for AISI 304 steel that brought about a sharper rise in temperature were reducing cutting time (spindle speed and feed per tooth). This is logical because they also reduce the time required to dissipate heat. Among these parameters, it was observed that employing a higher feed rate per tooth and a slower spindle speed led to a more marked increase in cutting temperature rather than the opposite effect, which corresponded to experiences indicated by other authors for high-speed machining conditions.

The parameter for the other two materials (ETP-R300 copper and aluminum alloy) that led to a more marked temperature rise was cutting depth. The parameters that shortened cutting time did not have much impact on cutting temperatures, and showed an overlap in the graphics.

Higher cutting temperatures were recorded in AISI 304 stainless steel machining due to this material's better resistance and to the increase that this resistance undergoes with deformation compared to other materials. The thermal conductivity of this material was very low, so heat concentrated more.

Lower temperatures were recorded for ETP-R300 copper milling. This could stem from the high thermal conductivity, which favored better heat transmission throughout the workpiece.

## Nomenclature

$a_e$ – radial depth, [mm]
$a_p$ – axial depth, [mm]
$C$ – specific heat, [$Jkg^{-1}K^{-1}$]
$K$ – thermal diffusivity, [$m^2s^{-1}$]
$N$ – spindle speed, [rpm]
$\Delta T$ – mean temperature, [°C]
$t_0$ – chip thickness before cut, [mm]
$U$ – specific energy in the operation, [$Nmmm^{-3}$]
$V_c$ – cutting speed, [$mmin^{-1}$]
$W_{BB}$ – radiation emitted by a blackbody
$W_{RB}$ – radiation emitted by a real body
$W_{emanating}$ – emanated radiation from an object
$W\varepsilon$ – emitted radiation coefficient
$W\rho$ – reflected radiation coefficient
$W\tau$ – transmitted radiation coefficient

*Greek symbols*

$\varepsilon$ – emissivity
$\rho$ – density, [$kgm^{-3}$]

## References

[1] Groover, M. P., *Fundamentals of modern manufacturing*, 4th ed., John Wiley and Sons, United States, 2010
[2] Kalpakijian, S. & Schmid, S., *Manufacturing processes for engineering materials*, 5th Education, Pearson, Naucalpan de Juarez, Mexico, 2007
[3] Nedić, B. P., Erić, M. D., Cutting Temperature Measurement and Material Machinability, *Thermal Science*, *18* (2014), 1, pp. 259-268
[4] Lazoglu, I., Altintas, Y., Prediction of Tool and Chip Temperature in Continuous and Interrupted Machining, *International Journal of Machine Tools and Manufacture, 42* (2002), 9, pp. 1011-1022
[5] Le Coz, G., *et al*., Measuring Temperature of Rotating Cutting Tools: Application to MQL Drilling and Dry Milling of Aerospace Alloys, *Applied Thermal Engineering, 36* (2011), Apr., pp. 434-441
[6] Wang, Z., *et al*., Energy Efficient Machining of Titanium Alloys by Controlling Cutting Temperature and Vibration, *Procedia CIRP, 17* (2014), July, pp. 523-528
[7] Erić, M., Nedić, B., Materials Machinability in Relation to the Cutting Temperature, *Tribology in Industry, 24* (2002), 3-4, pp. 79-82
[8] Davies, M. A., *et al*., On the Measurement of Temperature in Material Removal Processes, *CIRP Annals-Manufacturing Technology, 56* (2007), 2, pp. 581-604
[9] Armendia, M., *et. al*., High Bandwidth Temperature Measurement in Interrupted Cutting of Difficult to Machine Materials, *CIRP Annals- Manufacturing Technology, 59* (2010), 1, pp. 97-100
[10] Ansoategui, I., *et al*., Milling Simulation by Interrupted Cutting on Lathe to Measure Temperatures in the Cutting Tool (in Spanish), *XVIII Congreso Nacional de Ingeniería Mecanica*, Ciudad Real. Espania, 2010
[11] Grzesik, W., Experimental investigation of the Cutting Temperature when Turning with Coated Indexable Inserts, *International Journal of Machine Tools & Manufacture, 39* (1999), 3, pp.355-369
[12] Richardson, D. J., *et al*., Modelling of Cutting Induced Workpiece Temperatures for Dry Milling, *International Journal of Machine Tools and Manufacture, 46* (2006), 10, pp. 1139-1145
[13] Kuczmaszewski, J., Zagorski, I., Methodological Problems of Temperature Measurement in the Cutting Area during Milling Magnesium Alloys, *Management and Production Engineering Review, 4* (2013), 3, pp.26-33
[14] Pittala, G. M., Monno, M., A New Approach to the Prediction of Temperature of the Workpiece of Face Milling Operations of Ti-6Al-4V, *Applied Thermal Engineering, 31* (2011), 2-3, pp. 173-180
[15] Minkina, W. & Dudzik, S., *Infrared Thermography: Errors and Uncertainties*, 1st ed., John Wiley and Sons, London, 2009
[16] Lauro, C. H., *et al*., Monitoring the Temperature of the Milling Process Using Infrared Camera, *Scientific Research and Essays, 8* (2013), 23, pp. 1112-1120
[17] Dinc, C., *et al*., Analysis of Thermal Fields in Orthogonal Machining with Infrared Imaging, *Journal of Materials Processing Technology, 198* (2008), 1-3, pp. 147-154

[18] Valiorgue, F., *et al*., Emissivity Calibration for Temperatures Measurement Using Thermography in the Context of Machining, *Applied Thermal Engineering, 58* (2013), 1-2, pp. 321-326
[19] Cook, N. H., Tool Wear and Tool Life, *ASME Transactions, J. Eng. Ind., 95* (1973), 4, pp. 931-938
[20] Abukhshim, N. A., *et al*., Heat Generation and Temperature Prediction in Metal Cutting: A Review and Implications for High Speed Machining, *International Journal of Machine Tools and Manufacture*, *46* (2006), 7-8, pp. 782-800
[21] Garg, A., *et al*., Energy Conservation in Manufacturing Operations: Modelling the Milling Process by a New Complexity-Based Evolutionary Approach, *Journal of Cleaner Production, 108* (2015), Part A, pp. 34-45
[22] Bagavathiappan, S., *et al*., Online Monitoring of Cutting Tool Temperature During Micro-End Milling Using Infrared Thermography, *Insight, 57* (2015), 1, pp. 1-9

Paper submitted: January 26, 2016
Paper revised: May 14, 2016
Paper accepted: May 18, 2016